Magee Womens Research Institute and Foundation

Annual Progress Report: 2010 Formula Grant

Reporting Period

January 1, 2011 – June 30, 2011

Formula Grant Overview

The Magee Womens Research Institute and Foundation received $1,209,415 in formula funds for the grant award period January 1, 2011 through December 31, 2011. Accomplishments for the reporting period are described below.

Research Project 1: Project Title and Purpose

Analysis of Small RNAs in the Fetal Placental Maternal Interface - Small RNAs are present in the fetal and maternal circulations, and within the placenta. We recently found that maternal plasma microRNAs (miRNAs) inversely correlate with placental miRNAs. We surmised that small RNAs may serve as intercellular and systemic signals between the maternal and feto-placental compartments. To test the hypothesis that discrete miRNA species are transported across the maternal-placental-fetal interface, we will use next generation sequencing technologies to comprehensively define the expression of miRNAs and other small RNAs in the maternal plasma, placenta, and fetal blood, and deploy novel statistical-computational tools to interrogate the dynamic communication patterns of miRNA during human gestation.

Anticipated Duration of Project

1/1/2011 - 12/31/2011

Project Overview

Development of the eutherian embryo is utterly dependent on the placenta, which governs the exchange as well as communication between the blood of two organisms, taking place through a hemochorial layer of epithelial trophoblast and fetal endothelial cells. The expression of mRNAs and proteins are regulated by microRNAs (miRNAs) and other small RNAs in distinct spatial patterns. Although unique types of miRNAs have been validated in the human placenta, the contribution of these miRNAs to maternal plasma RNAs during pregnancy is unknown. Moreover, the expression and function of fetal miRNAs and small RNAs are unknown. We posit that exquisite expression patterns of miRNAs and small RNAs are germane for intact embryonic development and growth. We will first define the expression profiles of all miRNAs and small RNAs in the placenta and interfacing maternal and fetal blood during human pregnancy. Once we have the comprehensive expression data of all miRNA and small RNA species in the triad of human maternal blood, placenta, and fetal blood, we will use novel statistical analyses to interrogate dynamic changes in microRNA expression during human gestation prior to delivery,

and search for the patterns of miRNAs and small RNA communication among maternal blood, placenta, and fetal blood. Information gleaned from our data may not only illuminate epigenomic pathways that influence human embryonic development, but may also suggest innovative, clinically-relevant biomarkers, as well as preventive interventions designed to decrease the likelihood of injury before birth, thereby reducing the incidence of postnatal and adult diseases.

Specific Aims:

Aim 1: Define the expression profile of all miRNA and small RNA species in the maternal blood, placenta, and fetal blood at the end of human pregnancy using next generation sequencing technology.
Aim 2: Develop and apply novel statistical/computational tools to interrogate dynamic, coordinated patterns of miRNA and small RNA expression.

Project outcomes will be instrumental in suggesting a possible role for small RNA molecules in communication patterns among the maternal plasma, placenta, and the fetal blood.

Principal Investigator

Tianjiao Chu, PhD
Asst. Professor
University of Pittsburgh
204 Craft Ave.
B409
Pittsburgh, PA 15213

Other Participating Researchers

Yoel Sadovsky, MD - employed by University of Pittsburgh
Chunming Zhu, PhD, Ilya Goldin - employed by Magee-Womens Research Institute

Expected Research Outcomes and Benefits

After completing this project, we will define the microRNA expression profiles in the three compartments during human gestation prior to delivery, and establish the pattern of communication of microRNAs among maternal plasma, placenta, and fetal blood. Information gleaned from our data may not only illuminate epigenomic pathways that influence human embryonic development, but also suggest novel biomarkers and therapeutic approaches to obstetrical diseases stemming from placental dysfunction, which affect more than 10% of the annual four million deliveries nationwide.

It is also expected that results from the proposed studies will fuel additional research and submission of new grant proposals that center on the targets and regulation of miRNA and small RNAs in the placenta, fetal and maternal plasma.

Summary of Research Completed

As outlined in our research plan, in the first six months of this project we established the pipeline for the analysis of serum and placental miRNA as well as other small RNAs sequencing data. Using R programming language we also implemented the statistical algorithms used to test the presence and the change in expression of small RNAs (miRNA and unusually small RNA, usRNA) in the placenta, fetal blood, and maternal blood, and conducted a preliminary analysis using external data. Lastly, we have completed the attainment of an IRB approval to all components of materials necessary for our experiments, paving the way to the successful completion of our experiments in the second half of the funding period.

<u>Sequencing data analysis pipeline:</u>
We established a bioinformatics pipeline for the analysis of small RNA (microRNA and usRNA) sequencing data, and validated the pipeline using four small RNA libraries, generated from primary placental cells. The analysis pipeline consists of the following five steps:

1. Quality Assessment: FastQC is used to assess the overall quality of the sequencing libraries. In particular, the distribution of the quality scores across all bases, the sequence duplication level, as well as over-represented sequences are reviewed.
2. Adapter Removal: Based on the information provided by the sequencing service provider (Duke University), as well as results of FastQC assessment, adapter sequences for each library are identified and removed using the Bioconductor R package Biostrings. The 3'-end of each read is aligned against the 5'-end of the adapter sequence to identify the longest suffix of the read that matches a prefix of the adapter sequence, with up to 10% of bases allowed to be mismatches. The reads, with the accompanied quality scores, are then trimmed to remove the adapter sequence.
3. Align the Trimmed Reads: The trimmed reads, along with the trimmed quality scores, are aligned to human reference genome (ftp://ftp.1000genomes.ebi.ac.uk/vol1/ftp/technical/reference/human_g1k_v37.fasta.gz), using the short read aligner bowtie. Because of the shorter read length, only perfect alignments are allowed, and all perfect alignment are reported.
4. Annotate the Alignment: Ensembl annotation of all mRNA and non-coding RNAs are downloaded and converted to GFF format. Using BEDTools, the alignments, converted in BAM format, are intersected with the Ensembl annotation. Only alignments that overlap with Ensembl annotations are kept.
5. Calculate and normalize the "Weighted Count" of small RNAs: If one read has k genomic alignments that intersect with annotated mRNAs and/or noncoding RNAs in the Ensembl annotation, each intersecting alignment will be assigned a weighed count of 1/k. The sum of the weighted counts of all alignments from all reads intersecting with a miRNA in the Ensembl annotation is reported as the count of that miRNA. The weighted count of all miRNAs from all libraries then are normalized using the quantile normalization method.

We validated the sequencing data analysis pipeline using four small RNA libraries generated from the Primary Human Trophoblast (PHT) cells, dispersed from a single placenta. The PHT cells were separated into two plates. One plate was cultured under hypoxic condition (pO_2 <1%) for 48 hours. The other plate was treated under normoxic condition pO_2 = 20% for 48 hours.

From each plate, small RNAs 15 to 18 nucleotide long (putative usRNA) as well as small RNAs 19 to 30 nucleotides long (putative microRNA) were extracted separately. In total, four small RNA samples were extracted. The four samples were size fractionated using electrophoresis, barcoded libraries were generated and sequenced using Illumina HiSeq2000 sequencer at Duke University sequencing facility.

We successfully deployed our sequencing data analysis pipeline to the 4 Illumina libraries generated from the four samples. Figure 1 shows the quality scores across all 36 bases in the first library (15-18 nucleotides long RNA sample from PHT cells cultured under normoxic conditions). The figure shows that this library has overall very high quality scores across all 36 bases. Figure 2 represents a plot of the distribution of the length of sequences in the 4 libraries after the adapters have been trimmed. The X axis represents the length of trimmed reads, and the Y axis represents the percentage of reads in each library of a certain length.

External data analysis:
In addition to preparation and validation of the pipeline for the small RNA sequencing analysis, we also obtained an external data set of matched cord blood/placenta miRNA samples from 16 participants, from the University of Pennsylvania. These samples were collected by an NIH network that centers on genomic analysis of preterm births. Dr. Sadovsky, a co-investigator with Dr. Chu (PI), is a member of this network's steering committee. Expression levels of miRNA in these samples were measured using Affymetrix miRNA microarrays. The Robust Multi-array Average (RMA) method implemented in the Bioconductor R package was used to summarize and normalize the expression levels of the human miRNAs. We correlated the expression level of each placental miRNA to its expression level in the matched cord blood sample, and used the Fisher transformation to test the significance of the correlations. The p-values of these tests then were adjusted using the q-value method, implemented in R package qvalue, to control the false discovery rate. Our results indicated that the expression levels of none of the placental miRNAs significantly correlated with the corresponding miRNA in the cord blood. We believe that the lack of significant correlation was primarily caused by the high variability and "noise" in the Affymetrix miRNA microarray, as we observed high variation across the microarrays even for miRNAs with very high expression level.

To reduce the variance of the miRNA expression levels, we calculated for each miRNA its average log2 expression level over all cord blood samples and all placenta samples, respectively. Instead of calculating the correlation between cord blood and placenta for each miRNA, which becomes impossible given that we had only a pair of data points for each miRNA, we calculated the correlation for a group of human miRNAs. Specifically, we calculated the correlation for a set of miRNAs that are a part of the chromosome 19 miRNA cluster (C19MC) that are abundant in the placenta (log2 expression level > 9). In addition, we calculated the correlation for all other human miRNAs that are not a part of the C19MC miRNAs, and are abundant in placenta (log2 expression level > 9). We hypothesized that, in the presence of inter-compartment miRNA transport, the correlation for a set of miRNAs that are naturally expressed in one compartment would be stronger than those of miRNAs that are naturally expressed in both compartments, (this was implied in Equation 2 of our model for inter-compartment miRNA transport). Thus, because C19MC miRNAs are almost exclusively expressed in placenta (and at a high level), we predicted a stronger correlation for the set of C19MC miRNAs between the placenta and cord blood, than

other miRNAs. Indeed, the correlation of C19MC miRNA between cord blood and placenta was extremely strong (0.74). The correlation of other miRNAs between cord blood and placenta was markedly lower (0.26, which is significantly less than that of C19MC, p value < 0.05). Figure 3 shows the average log2 expression level of all human miRNAs in cord blood (X axis) and placenta (Y axis). The red dots represent the C19MC miRNAs, and the blue dots represent other miRNAs. It is clear from the plot that C19MC miRNAs show a much stronger correlation between cord blood and placenta.

Summary:

During the first six months of the project we successfully established and validated a pipeline for small RNA (miRNA and usRNA) sequencing data analysis, and implemented a statistical test procedure for the detection of miRNA transport in R. We also obtained IRB approval for our protocol, paving the way to full data collection. We also performed a preliminary data analysis using external data. Despite a high overall level of variability using the Affymetrix miRNA arrays, we designed an alternative strategy, and we were able to support the notion that some miRNAs indeed transport between the placenta and cord blood.

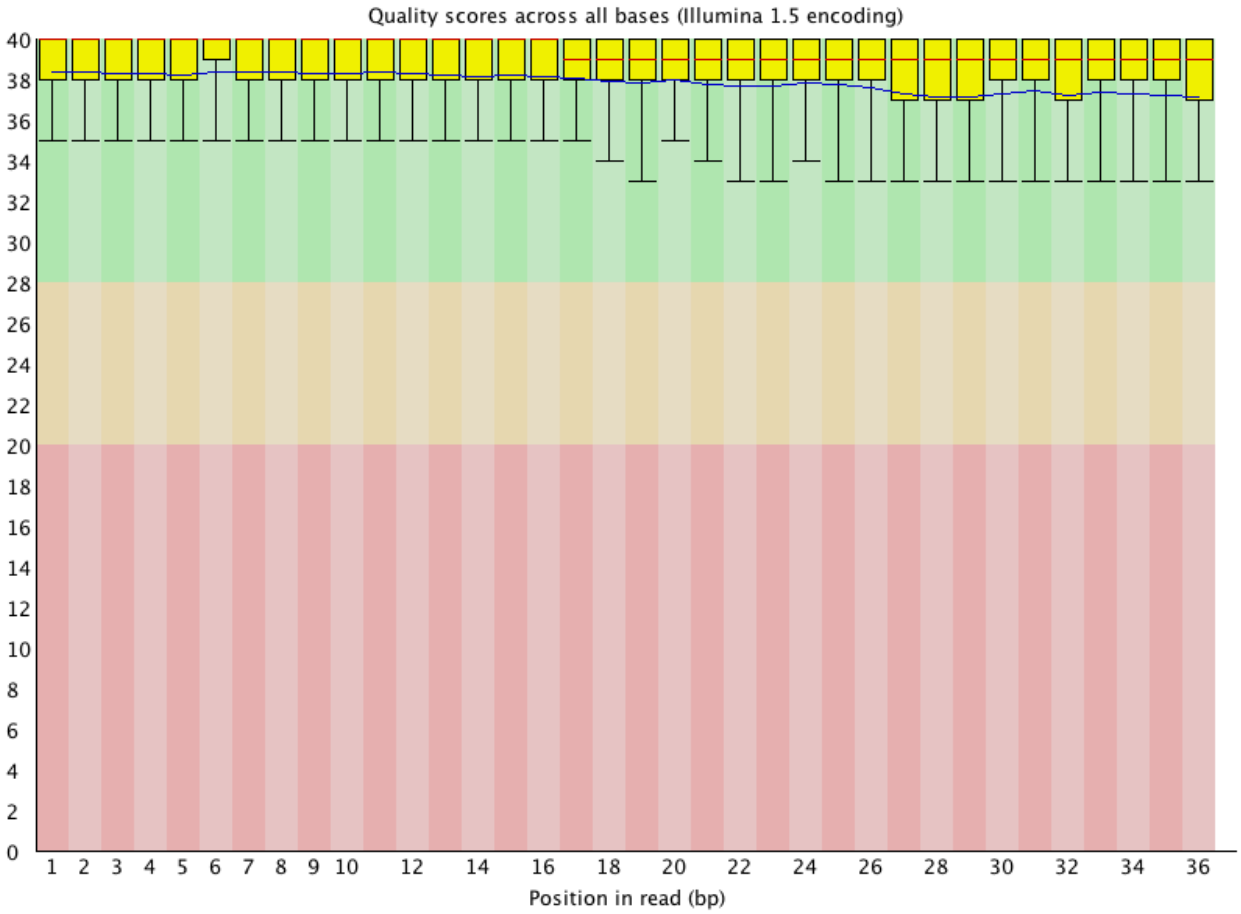

Figure 1: Quality Score Assessment of our Illumina Library. The X axis represents the positions on the 36bp reads. The Y axis represents the Phred quality score, which is defined as -10 * log10 (Probability of base call error). The higher the Phred score, the higher the quality of a base call.

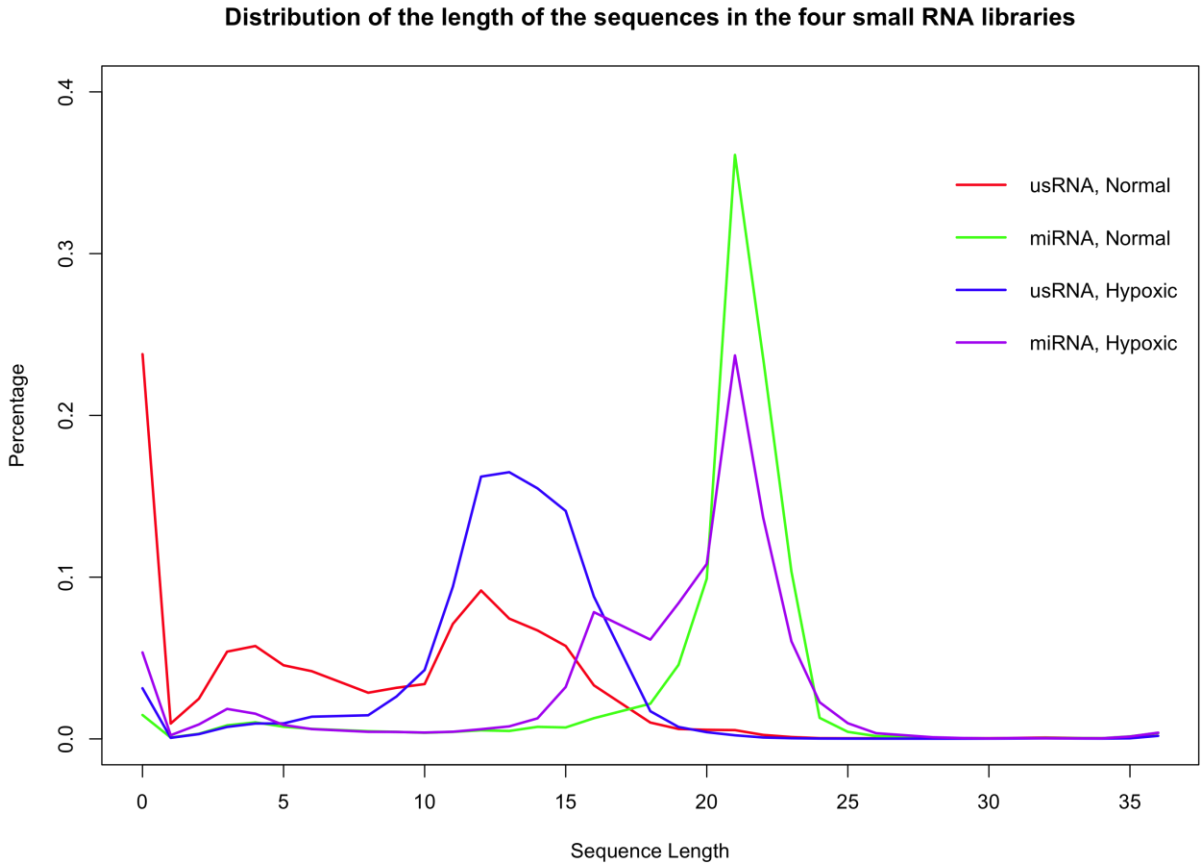

Figure 2. Length Distribution of the Trimmed Reads in Four Small RNA Libraries. The X axis represents the length of trimmed reads. The Y axis represents the frequency of the trimmed reads (percentage). The four curves represents four small RNA libraries. The usRNA in the label refers to the samples of RNA between 15 to 18 nucleotides long, and miRNA refers to the samples of RNA between 19 and 30 nucleotides long.

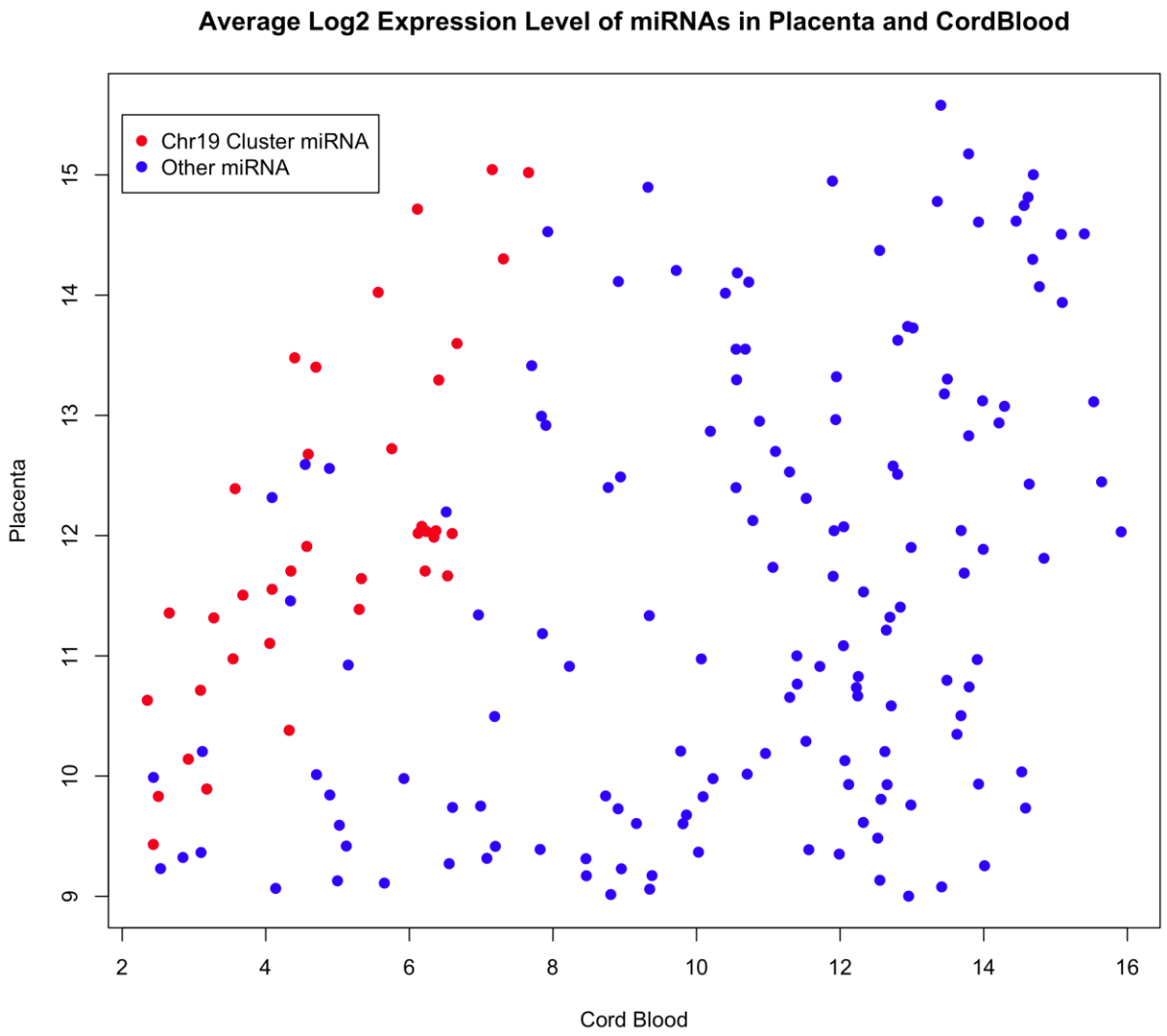

Figure 3. Average Log2 Expression Level of miRNAs in Matched Cord Blood and Placenta Samples. The X axis represents the average log2 expression of the miRNAs in the 16 cord blood samples. The Y axis represents the average log2 expression of the miRNAs in the 16 matched placenta samples. Red dots represent C19MC miRNAs. Blue dots represent all other miRNAs. Only miRNAs with average log2 expression level > 9 in placenta are plotted.

Research Project 2: Project Title and Purpose

miR-210 Regulation of Mitochondria Function - We plan to characterize the function of a hypoxia inducible microRNA, miR-210, in ovarian cancer oncogenesis, especially the mechanism of miR-210 regulating mitochondria metabolism and its contribution to ovarian cancer initiation and progression. By completing this study, we hope to establish miR-210's role in ovarian cancer and identify novel miR-210 target genes as potential targets for ovarian cancer therapy.

Anticipated Duration of Project

1/1/2011 - 12/31/2011

Project Overview

The main objective of this project is to illustrate the biological function of miR-210 in ovarian cancer and its potential for ovarian cancer therapy. We propose a series of mechanistic studies to investigate miR-210's function in ovarian cancer, especially its contribution to ovarian cancer energy metabolism under hypoxic conditions. Specifically, we will examine miR-210's copy number in a variety of ovarian cancer cell lines using fluorescence in situ hybridization (FISH) and corresponding miR-210 expression in these cell lines to correlate its copy number with gene expression level. Subsequently, we will ectopically express miR-210 in at least two ovarian cancer cell lines to examine miR-210's expression on ovarian cancer cell survival, proliferation, apoptosis, and metabolism. In addition, we will verify our computationally predicted miR-210 target genes in mitochondria metabolism pathways by Argonaute 2 immunoprecipitation followed by real-time polymerase chain reaction (PCR) assays and by Western Blotting. We will also investigate the function of miR-210 target genes on mitochondria function by overexpressing and knocking down the genes on energy metabolism, oxygen consumption, and cell survival and proliferation. Finally, we will examine the expression of miR-210 and its target gene in banked clinical specimens to correlate its expression with tumor hypoxia and ovarian cancer patient clinical outcomes. In summary, this project is intended to provide mechanistic insights on miR- 210's function in ovarian cancer and to explore the possibility to target miR-210 pathway for ovarian cancer therapy.

Principal Investigator

Xin Huang, PhD
Assistant Professor
Magee-Womens Research Institute
B601, MWRI
204 Craft Ave.
Pittsburgh, PA 15213

Other Participating Researchers

Chong Da Tan, Joan Brozick - employed by Magee-Womens Research Institute

Expected Research Outcomes and Benefits

Epithelial ovarian cancer (EOC) is the fifth leading cause of cancer death in women in the United States and currently, there is no effective therapy for late stage EOC. Our project will address the function of miR-210 in EOC cells. We expect to identify the role miR-210 plays in ovarian cancer cell energy metabolism by genetic and biochemical approaches and verify its target gene in clinical specimens by immunohistochemistry (IHC), real-time PCR, and Western blotting. miR-210 and its target gene identified in this study may provide novel therapeutic targets for EOC treatment.

Summary of Research Completed

We have determined the copy number of miR-210 in 13 ovarian cancer cell lines and miR-210 expression in 12 ovarian cancer cell lines. We have also identified a subunit of mitochondria electron transport chain (ETC) Complex I, NDUFA4, as a new miR-210 target gene. Our data suggest that miR-210 may be a master regulator of cellular energy metabolism under hypoxic conditions. Here, we summarize our findings to date:

<u>miR-210 is deleted in high frequency in ovarian cancer cells</u>

As proposed in our Aim #1, we determined miR-210 copy number in 13 ovarian cancer cell lines using a bacterial artificial chromosome (BAC) clone, RPCI11-496I9 that include the entire genomic region of miR-210. We labeled the BAC DNA in red and chromosome 11 centromere probe with green and performed fluorescence in situ hybridization (FISH) to measure miR-210 copy number. We observed miR-210 loss in at least 30% of cell population in eight of thirteen ovarian cancer cell lines examined (61%). Interestingly, the vast majority of miR-210 copy number loss is single copy loss and no homozygous deletion was detected (Fig. 1A), suggesting that miR-210 may not be a target of chromosome 11p15.5 deletion. In order to confirm this, we also performed RT-qPCR to estimate miR-210 baseline expression or hypoxia induction in 12 ovarian cancer cell lines. No direct correlation between miR-210 copy number and miR-210 baseline expression or hypoxia induction was observed (Fig. 1B).

<u>NDUFA4 is a miR-210 target</u>

Because miR-210 is highly induced under hypoxic conditions, we searched for its target genes that may be involved in cellular response to hypoxic stress. It's well known that under hypoxic conditions, cells upregulate glycolysis by HIF1α to meet cellular energy demand due to diminished oxygen availability. However, how cells downregulate oxidative phosphorylation (OXPHOS) is less clear. We found that NDUFA4, a subunit of mitochondria ETC Complex I, is a potential miR-210 target gene, which may explain how cells downregulates OXPHOS. We cloned the 3' UTR of NDUFA4 into a luciferase reporter vector and performed reporter assay with co-transfected miR-210 expressing construct. As shown in Fig. 2A, the luciferase activity

can be specifically downregulated by overexpressing miR-210, indicating NDUFA4 is a miR-210 target. We have also overexpressed miR-210 in SKOV3ip.1 cells and observed downregulation of endogenous NDUFA4 protein (Fig. 2B). When miR-210 is knocked down under 2% oxygen, NDUFA4 repression by hypoxia can be partially rescued (Fig. 2C), further supporting our conclusion that NDUFA4 is a miR-210 target.

NDUFA4 is a specific mitochondria target of hypoxia

Because miR-210 is highly induced under hypoxia, we asked whether NDUFA4 expression is repressed under hypoxic condition. We collected a variety of cell lines from different origins and performed Western blotting. Strikingly, NDUFA4 expression is essentially completely repressed in all cell lines examined (Fig. 3A), suggesting NDUFA4 regulation under hypoxia is a general mechanism for cells to downregulate OXPHOS. In order to examine whether hypoxic regulation of NDUFA4 is specific for Complex I subunits, we randomly selected three other subunits of Complex I for Western blotting analysis. Fig. 3B indicates that only NDUFA4 is specifically repressed by hypoxia, further suggesting that NDUFA4 may be the target of hypoxia regulation of mitochondria function. Currently, we are performing functional assays to examine mitochondria function under hypoxia and after miR-210 overexpression/NDUFA4 knockdown.

A.

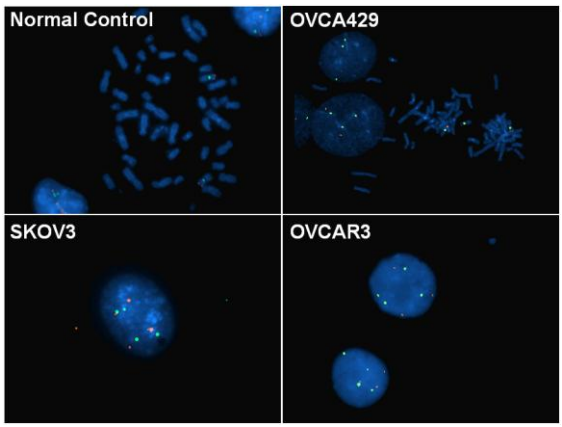

	Normal	Loss	Gain
OVCA420	4%	96%	
OVCA429	2%	98%	
OVCA432	49%	51%	
OVCA433	2%	98%	
A2780	93%	3%	4%
CP70	92%	5%	3%
OVCAR3	2%	98%	
SKOV3	95%	5%	
MESOV	93%	3%	4%
IGROV1	69%	31%	
OVCAR8	27%	73%	
HEYA8	69%	31%	
ES2	75%		25%

B.

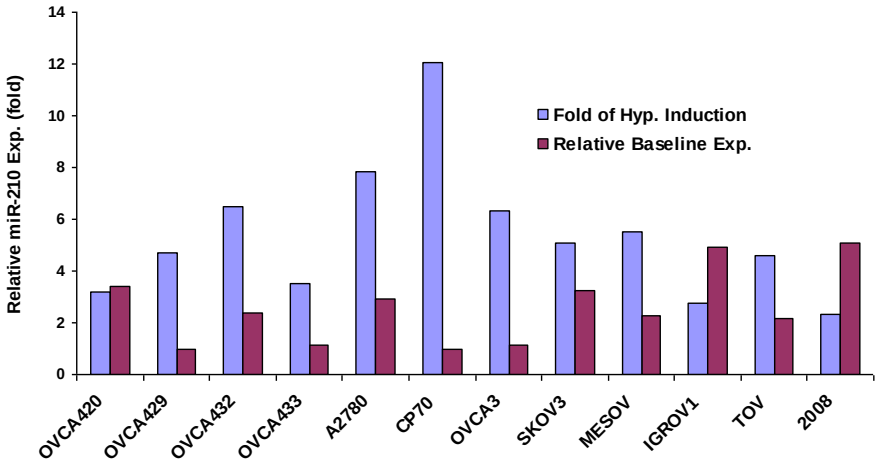

Figure 1. miR-210 copy number and expression is not correlated in ovarian cancer cells. (A) miR-210 is lost at high frequency in ovarian cancer cells. Left panel, representative images of miR-210 FISH; Right panel, summary of miR-210 FISH results in 13 ovarian cancer cell lines. (B) miR-210 baseline expression and hypoxia induction is robust and does not correlate with its copy number.

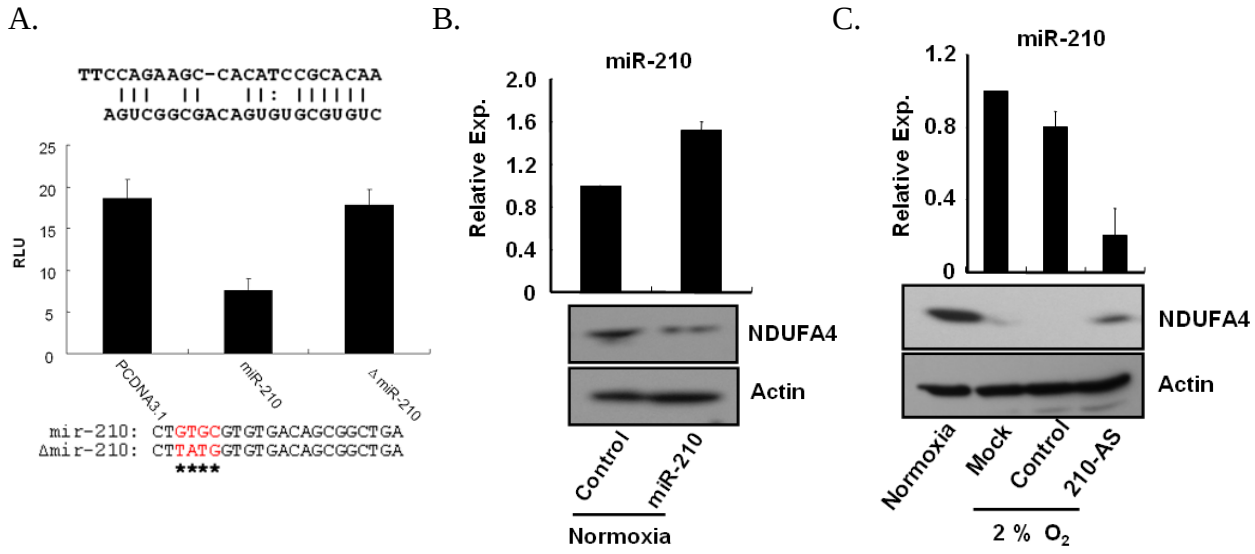

Figure 2. NDUFA4 is a miR-210 target. (A) miR-210 can repress luciferase reporter activity by interacting with NDUFA4 3' UTR cloned at downstream of the luciferase reporter gene. When miR-210 "seed region" is mutated, the repression is abolished. Top panel, the putative binding between miR-210 and NDUFA4 3' UTR. Bottom panel, the mutation of miR-210 "seed region" in the miR-210 expression construct. (B) Ectopic expression of miR-210 can downregulate endogenous NDUFA4 expression. (C) Knockdown of miR-210 expression at 2% oxygen by locked nucleic acid (LNA) oligo against miR-210 can partially rescue NDUFA4 expression.

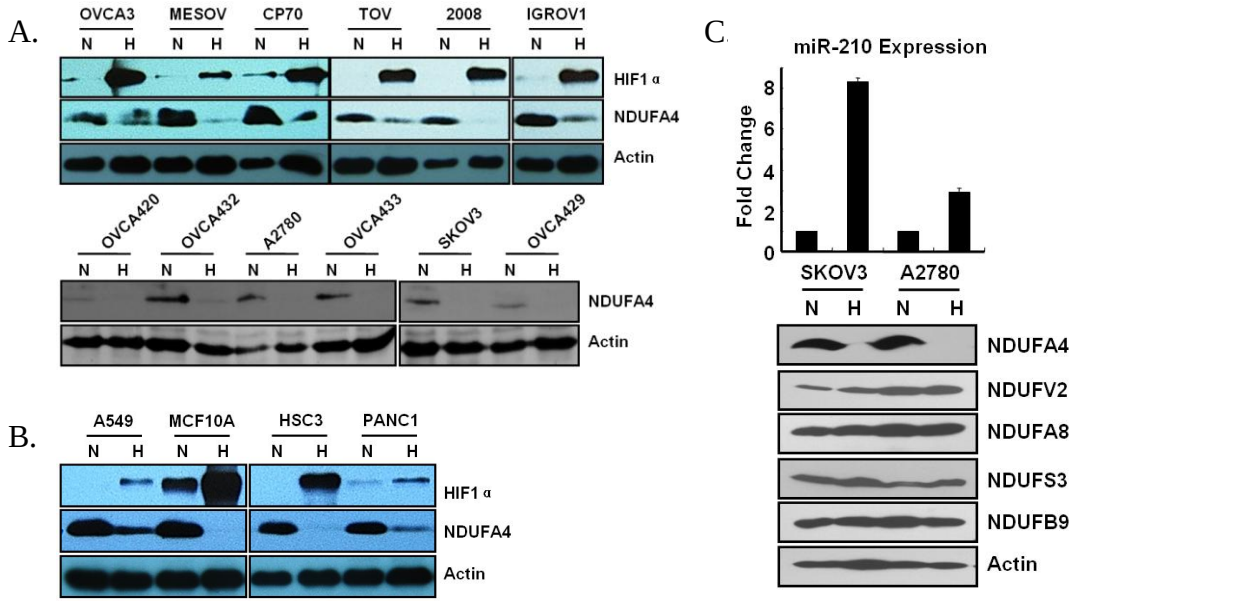

Figure 3. NDUFA4 expression is repressed by hypoxia. (A) NDUFA4 expression is repressed by hypoxia in ovarian cancer cell lines. (B) NDUFA4 expression is repressed by hypoxia in a variety of cell lines from different origins, including A549, lung cancer; MCF10A, immortalized breast cells; HSC3, head & neck cancer cells; PANC1, pancreatic cancer cells. (C) NDUFA4 is a mitochondria ETC Complex I subunit that is specifically repressed by hypoxia.

Research Project 3: Project Title and Purpose

Functional Analysis of the C19MC MicroRNAs in Trophoblasts - Our goal is to better understand placental physiology and the causes of placental insufficiency leading to gestational diseases. MicroRNAs have emerged as critical regulators of virtually every biological process and their altered expression is increasingly found associated with pathological states. Recently, it was found that the placenta is the exclusive source of a large family of miRNAs originating from a unique cluster located on chromosome 19 (C19MC). While the expression of these miRNAs is normally restricted to placental trophoblasts, their aberrant expression in other cell types is often associated with malignant conditions. However, the relevant biological function of these miRNAs in the placenta remains poorly understood. In this project, we propose to investigate the function of the C19MC miRNAs in trophoblast cells.

Anticipated Duration of Project

1/1/2011 – 12/31/2011

Project Overview

Placental insufficiency is one of the main complications of pregnancy and is associated with compromised fetal development and poor outcome. These pathologies are thought to stem from inadequate placental development but the molecular mechanisms underlying placental insufficiency remain poorly understood. The discovery of miRNAs and the realization that miRNAs are abundant in the human placenta offer new perspectives on placental development and pathophysiology. Consistent with this, mutations that disable the miRNA biogenesis machinery lead to impaired placental development. In addition, miRNA expression profiling experiments performed in placentas from patients with preeclampsia have shown anomalies in miRNA expression patterns compared to uncomplicated pregnancies.

One of the most notable observations about placental miRNAs is the abundance of highly related miRNAs that originate from a unique large cluster termed C19MC, encoding at least 48 mature mRNAs. Added to the fact that each miRNA can possibly target several hundred transcripts, the combined regulatory potential of these miRNAs is huge. The biological role of these abundant miRNAs is unknown but several reports indicate that their aberrant expression can have dramatic cellular consequences such as cancer.

The overall aim of this project is to shed light on the role of the C19MC miRNAs in trophoblasts as they could be instrumental for placental morphogenesis and function. To test this hypothesis, we will first use a loss-of-function approach in primary trophoblasts and investigate the cellular consequences of suppressing the function of several members of these miRNAs. In the second specific aim we will focus on the molecular targets of these miRNAs and use microarrays to determine the impact of C19MC miRNAs on gene expression and identify mRNA targets in a trophoblast cell line.

Principal Investigator

Jean-Francois Mouillet, PhD
Instructor
University of Pittsburgh
Department of OBGYN and Reproductive Sciences
Magee-Womens Research Institute
204 Craft Avenue
Room A634
Pittsburgh, PA 15213

Other Participating Researchers

Yoel Sadovsky, MD, Tianjiao Chu, PhD, Elena Sadovsky-employed by University of Pittsburgh

Expected Research Outcomes and Benefits

Our long-term goal is to understand the response of the human placenta to injury, and in particular to low oxygen (hypoxic) stress. Low placental oxygenation is one of the main stress conditions in the human placenta and is believed to play a role in the development of pathologies such as intrauterine growth restriction (IUGR) and hypertension of pregnancy. These conditions are associated with increased perinatal illnesses and mortality. Newborns surviving these insults are at risk for lifelong complications, including developmental diseases and a greater incidence of the adult metabolic syndrome (type-2 diabetes, high lipids, hypertension, obesity and related illnesses). While these complications often originate from impaired placenta function, the molecular mechanisms involved remain elusive. A prerequisite to a better understanding of these gestational pathologies is the identification of the genes that play a role in the morphogenesis and function of the placenta. The recent recognition of microRNAs (miRNAs) as critical regulators of development and homeostasis and the discovery of miRNA abundance in the placenta have stimulated research routes that target the molecular underpinnings of placental insufficiency. We recently showed that miRNA expression was altered in placental trophoblasts that are exposed to hypoxic stress, which often leads to placental injury. We also demonstrated that the dysregulation of these miRNAs had the potential to affect cardinal regulators of placental development. Additionally, a family of placenta-specific miRNAs that originate from a single large cluster of miRNA genes located on human chromosome 19 (C19MC) was recently described. While highly expressed in trophoblasts, the role of miRNAs from the C19MC cluster and their impact on cellular function is unknown. The analysis of C19MC miRNA function will illuminate molecular pathways governing trophoblast differentiation and function. Furthermore, conclusions from our studies may uncover important mechanisms that contribute to placental dysfunction.

Summary of Research Completed

The human placenta is a unique source of a large family of microRNAs (miRNAs) that is encoded by a cluster on chromosome 19. Collectively, these miRNAs, referred to as chromosome 19 miRNA cluster (C19MC miRNAs), are the most abundant miRNAs present in placental trophoblasts and hold huge gene regulatory potential. To date, their function remains completely unknown. This project was undertaken in order to gain insight into the role of the C19MC miRNAs in the biology of placental trophoblasts. We report here on our progress, made during the first six funded months of this project.

Aim 1: Inhibit selected C19MC miRNAs and analyze functional consequences in primary human trophoblasts.

We originally planned to inhibit members of the C19MC miRNAs using specific decoys termed miRNA sponges. The technique is based on the forced expression of RNAs containing complementary sequences to a given miRNA species, causing the sequestration of the targeted miRNA and suppression of silencing of endogenous cellular targets. We generated a series of constructs harboring 4, 8, and 16 copies of target sequences for a miRNA of interest that were cloned into a pcDNA3 vector downstream the cytomegalovirus (CMV) promoter. Upon transfection in cells, these constructs produce a high number of transcripts that could potentially bind targeted miRNAs and lead to inhibition of the targeted miRNA. To monitor the efficiency of this approach, sponge constructs were cotransfected with a miRNA-responsive luciferase reporter (termed sensor). We first tested this experimental approach in a cell line (HTR-8Sv/Neo cells) before applying it to more challenging primary human trophoblasts. Transfection of increasing amounts of miRNA sponge in HTR-8Sv/Neo cells resulted in a consistent increase of luciferase activity, which we interpreted to reflect a relief of miRNA-mediated silencing of the reporter. However, the effect was rather modest, with a 20% or less increase of luciferase activity. Despite attempts to optimize various parameters we were not able to significantly increase the inhibiting power of these sponges. We determined that this magnitude of effect was insufficient for biologically meaningful inhibition of the C19MC miRNAs in primary human trophoblasts.

As an alternative to block members of the family of C19MC miRNAs, we decided to use synthetic anti-sense oligonucleotides that are delivered into cells by transfection. Several species from the cluster were selected on the basis of their expression levels, their location within the cluster, and seed sequence. A total of 7 different miRNA species were selected for functional inhibition, and subjected to knockdown experiments using Locked-Nucleic-Acid (LNA)-based oligonucleotide inhibitor from Exiqon (Denmark). These chemically-modified oligonucleotides have enhanced affinity and stability compared to regular DNA oligonucleotides, and have demonstrated efficiency in several cellular systems. We recently tested several formulations for anti-sense miRNA inhibitors from a variety of manufacturers and found that the miRCURY LNA™ microRNA Power Inhibitors from Exiqon exhibited the highest efficiency in our primary human trophoblasts.

These miRNA inhibitors (also called antagomirs) were transiently transfected into primary human trophoblasts using the transfection reagent DharmaFect 1 from Dharmacon. At 48h after

transfection we observed a substantial depletion of most of the selected miRNAs determined by quantitative real-time polymerase chain reaction (RT-PCR) of individual targeted miRNA (Fig.1). As an additional control of the inhibition of the targeted miRNA we performed another series of transfections in which specific miRNA sensor constructs were transfected along the antagomir. Each miRNA sensor construct is based on the psiCHECK2 vector (Promega) containing three artificial miRNA target sites. Upon transfection of the antagomir, the silencing of the luciferase reporter should be attenuated and luciferase activity increased. We observed some variability in the efficiency of the antisense inhibitors, yet all caused a major de-repression of the luciferase sensor activity (Fig.2), indicating an efficient knockdown of the targeted miRNAs. Despite the significant reduction of C19MC miRNA levels we did not observe any phenotypic consequences on the cultured primary trophoblasts. In particular, cytotrophoblast differentiation into syncytiotrophoblast did not appear to be affected by the depletion of individual C19MC miRNAs, as measured by the levels of hCG production. Transfected cells were also challenged by exposure to hypoxia (O_2 <1%), but upon initial analysis no marked phenotypic differences were observed in C19MC miRNA-depleted trophoblasts. We posited that partial inhibition of discrete C19MC miRNAs might alter the expression of only some target genes and result in subtle differences that may not translate into an obvious phenotype. We therefore performed a series of microarray experiments to determine the impact of inhibition of discrete C19MC miRNA species on gene expression. Total RNAs were extracted from primary trophoblasts transfected with a miRNA inhibitor or a scramble oligonucleotide and were hybridized to a SurePrint G3 Human GE 8x60k microarray. These experiments are now completed, and the results are being informatically analyzed.

Aim 2: Analyze gene expression in cells that ectopically express the C19MC miRNAs.

Experiments performed in the first aim of the project were designed to study the function of individual C19MC miRNAs in trophoblasts by interfering with the expression of single members of the cluster. In the second phase, we sought to investigate the role of the whole C19MC cluster in trophoblast gene expression, using stably transfected cells that ectopically express the entire C19MC locus.

Northern blot analyses performed in our laboratory showed that HTR-8Sv/Neo cells were the only trophoblast-derived cell line (among JEG3, BeWo, and JAR) that were deficient in C19MC miRNA expression. We reasoned that exogenous expression of these miRNAs in HTR-8Sv/Neo cells and comparison of gene expression patterns with non-expressing parental cells would provide us with a model system for studying the global impact of these miRNAs on the transcriptome.

We identified a bacterial artificial chromosome (BAC) clone covering the entire C19MC locus, using the University of California, Santa Cruz (UCSC) genome browser and purchased it from the “BACPAC Resource Center" (BPRC) located at the Children's Hospital Oakland Research Institute (CHORI). The BAC (clone #: RP11-1055O17) was then modified by recombineering in order to insert a zeocin selection cassette and the traceable GFP reporter gene. To do that, we first PCR amplified a GFP::zeocin cassette from the pSELECT-GFPzeo-mcs plasmid (InvivoGen, CA), and cloned it into the *Hind* III and *Bam* HI sites of pBluescript II SK(+) (pBS-SK). We then PCR amplified BAC specific homology arms of ~500 bp each and cloned them

into pBS-SK using the restriction sites flanking the GFP::zeocin cassette (5'arm: *Xho* I and *Hind* III; 3'arm: *Bam* HI and *Xba* I). The whole targeting cassette was then PCR amplified, gel purified, and electroporated into the recombinogenic SW106 bacterial strain containing the recipient BAC. Using this approach we generated two BAC constructs (Fig. 3): In addition to the construct that was simply tagged with the GFP::zeocin cassette at the 3'end of the C19MC cluster (BAC-C19-WT-GFP) we also created a BAC with a deletion of the sequence encoding all the miRNAs from the cluster and intended to be used as control in our transfection experiments. By choosing a 5' homology arm located upstream of the miRNA cluster and keeping the same 3' homology arm, the recombination led to the actual deletion (BAC "trimming") of the entire miRNA locus (~100 kb). The construct is referred to as BAC-C19-Del-GFP and contain ~60 kb of genomic DNA flanking the GFP::zeocin cassette. Bacteria harboring the BAC with the desired alteration were selected on selective medium with chloramphenicol (12.5 μg/ml) and zeocin (25 μg/ml). We further confirmed that the modified BAC contained the intended recombination by restriction mapping (Fig. 4) and PCR. At this stage the correct BAC construct was transformed back into DH10B bacterial cells for propagation.

We are currently in the process of optimizing the transfection method to introduce the modified BAC into HTR-8Sv/Neo cells. BAC DNA for transfection was isolated using the PhasePrep BAC DNA kit (Sigma) following the manufacturer's recommendations. To deliver the BAC DNA into the cells we first tested the kit Targefect-BAC (Targeting Systems). The kit combines a transfection reagent (Targefect-2) with a viral enhancer (Virofect). Pilot experiments using this system resulted in low transfection efficiency. We therefore elected to modify the method and use instead polyethyleneimine (PEI) as a DNA condensing agent and Virofect as an enhancer. This combination led to a substantial improvement of the transfection efficiency, which now reaches 10-20%.

In order to rapidly determine whether the C19MC miRNAs are expressed in transfected HTR-8Sv/Neo cells we set up an RT-PCR assay to detect transcripts originating from this region. The sequences of the primers are based on expressed sequence tags (ESTs) that are specifically expressed in the placenta and are known to originate from the C19MC locus. We first tested the assay using RNA from several cell lines (HTR-8Sv/Neo, JAR, JEG3, and HeLa) as well as two human tissues (prostate and placenta). A band of the expected size was uniquely amplified in JAR and JEG3 cells but not in HeLa or HTR-8Sv/Neo cells (Fig. 5). In tissues the band signal was detected only in the placenta sample, thus confirming assay specificity. Total RNA from transfected HTR-8Sv/Neo cells was isolated and used to interrogate C19MC expression using our RT-PCR assay. Figure 6 shows the presence of the band signal only in transfected cells, which clearly indicate that the transfected BAC is transcribed in HTR8 cells. We are now in the process of establishing stable HTR-8Sv/Neo cells expressing the C19MC miRNAs, thus expecting that all cells will express the transgene.

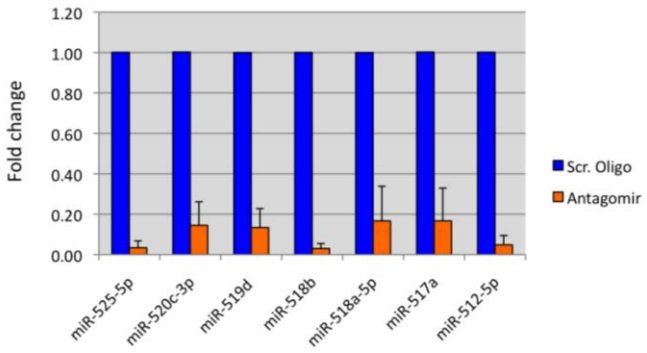

Fig. 1: The effect of antisense miRNA inhibitor on endogenous C19MC miRNAs in primary human trophoblasts. Cells were transfected with the indicated antisense oligonucleotide or a scramble oligonucleotide as a control. Targeted miRNAs levels were analyzed by real-time PCR. Data represent the mean of three independent experiments, performed in duplicate.

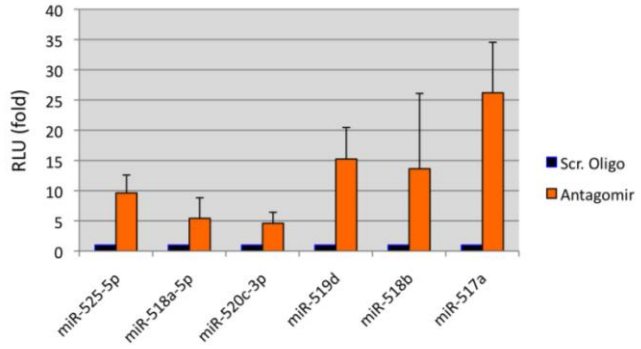

Fig. 2: The effect of antisense miRNA inhibitors on the activity of a luciferase reporter. Trophoblasts were transfected with one of the miRNA sensor constructs along with the corresponding targeting antisense oligonucleotide or a scramble oligonucleotide as a control. Relative luciferase unit (RLU) activity was determined 48 h later. Data represent the mean of three independent experiments, performed in duplicate.

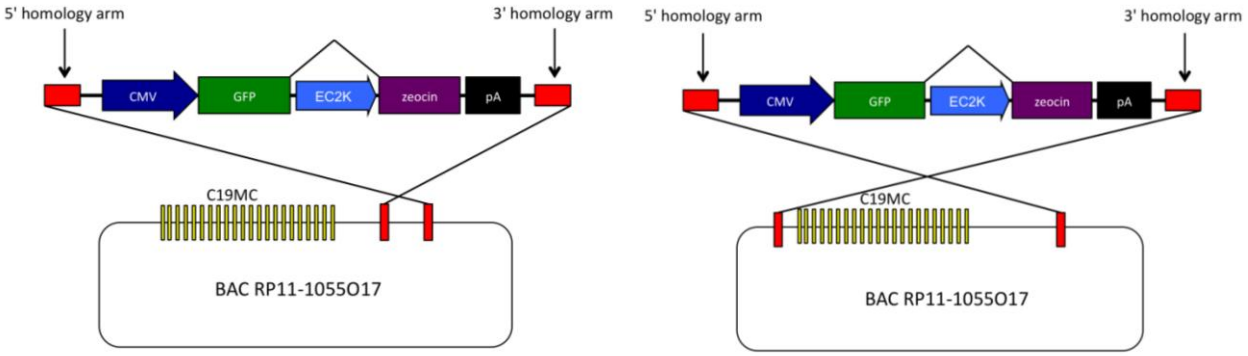

Fig. 3: Schematic representation of the BAC and the recombineering strategy. The left panel depicts the approach to insert the tagging cassette into the C19MC miRNA expression BAC. The right panel shows the BAC "trimming" that permits the insertion of the tagging cassette while removing the sequence coding the C19MC miRNAs.

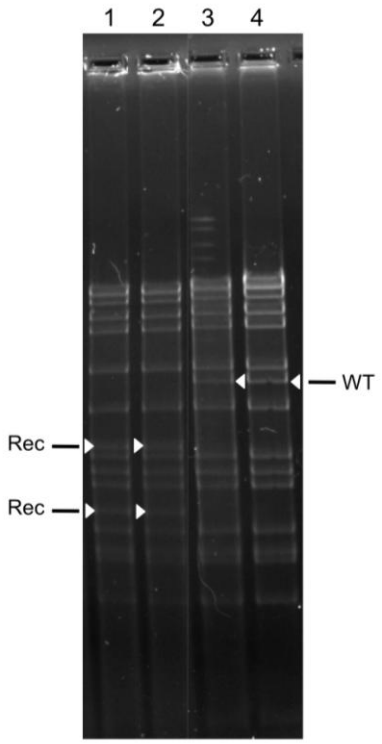

Fig. 4: Restriction analysis of modified BAC clones (example with BAC-C19-WT-GFP). BAC DNA was double-digested with Not I/Bam HI and separated by electrophoresis. Clones 1 and 2 have the desired modification while clones 3 and 4 correspond to the original unmodified BAC. After correct recombination one of the digestion bands in the original BAC (WT) is split in two (Rec) as a consequence of the insertion of the tagging cassette.

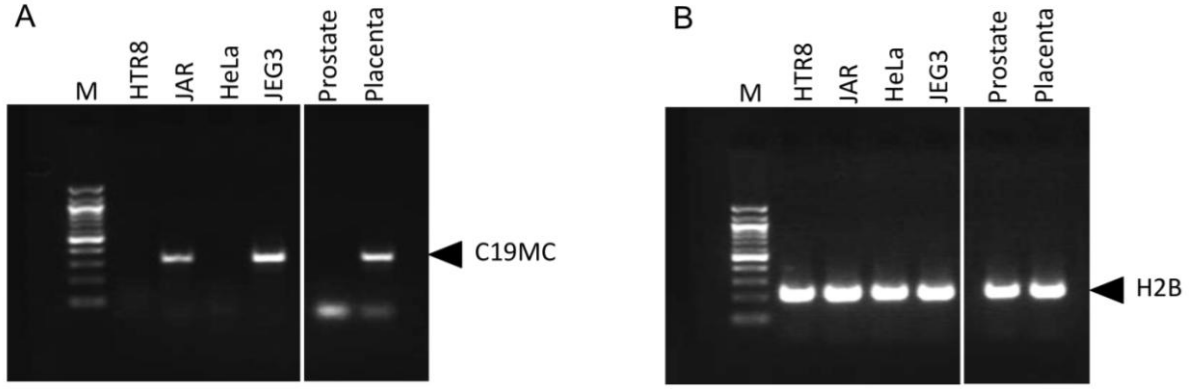

Fig. 5: RT-PCR analysis in human cell lines and tissues. The cDNA was prepared using the high capacity RNA to cDNA Master Mix (Applied Biosystems) and subsequently used in PCR. (A) RT-PCR of transcripts expressed from the C19MC cluster. Note the presence of C19MC-specific transcripts in placenta-derived cells (JAR and JEG3) with the exception of HTR-8Sv/Neo cells. (B) RT-PCR analysis of a housekeeping gene histone 2B (H2B) used as a control.

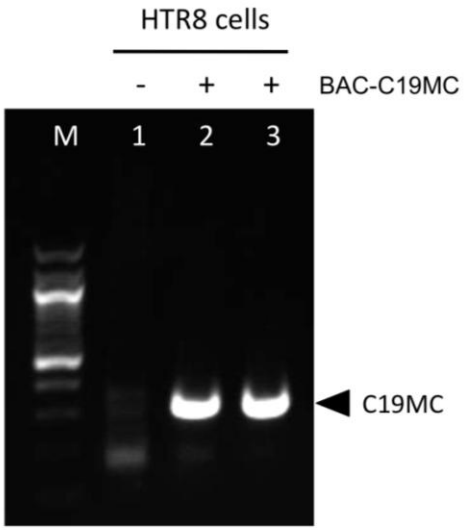

Fig. 6: RT-PCR analysis of parental HTR-8Sv/Neo cells and cells after transfection with the modified BAC plasmid. HTR8 cells were transiently transfected with a BAC-C19-WT-GFP and total RNA were isolated 48h later. The cDNA was prepared using the high capacity RNA to cDNA Master Mix (Applied Biosystems) and subsequently used in PCR for amplification of C19MC-specific transcripts. Lane 1 corresponds to mock-transfected cells. In lanes 2 and 3, the cells were transfected with the BAC containing the intact C19MC locus.

Research Project 4: Project Title and Purpose

Microtubule Post-Translational Modifications and Centrosome Dynamics During Mitosis in Normal and Cancerous Cells - Microtubule defects and centrosome aberrations cause cancers and birth defects, since they induce chromosome aneuploidies after mitosis in both somatic and embryonic cells. They are responsible for inherited disorders and their functioning is essential for brain activities. Consequently, their activities span life from conception through death. While cell biologists a century ago were as familiar with the centrosome ('the cell's central body') as they were with chromosomes ('the cell's colored bodies' because they bind cytological stains), progress in characterizing the molecular constituents and mechanisms responsible for functional activities has paled when comparing centrosome molecular biology with chromosome molecular biology. Nevertheless, the essential roles of the centrosome for normal cell function are now incontrovertible and a panoply of diseases and disorders result from microtubule and centrosome dysfunctions or 'centrosomopathies.' In this project we will characterize the vital permanent molecules in the mitotic centrosome and discover which reside temporarily at the centrosome, along with the post-translational modifications of microtubules which occur during normal and cancerous cell cycles.

Anticipated Duration of Project

1/1/2011 - 12/31/2011

Project Overview

In this project, we will examine the following specific aims with the objective to first define the basic molecular targets and later explore inhibitors which might uniquely target cancerous cells.

1. Do cancer cells display differences in the delta-2 post-translational modification of alpha-tubulin as compared with noncancerous cells?

2. Using dynamic confocal imaging with a living marker for centrioles, does GFP-centrin behave aberrantly in cancer cells as compared with controls?
3. Do the molecules which reside at the centrosome differ between cancer cells and controls?
4. Do the anticancer drugs currently used target these posttranslational modifications of alpha tubule, centrioles and/or these centrosomal molecular and can new drugs be discovered?

Principal Investigator

Calvin Simerly, PhD
Research Associate Professor
University of Pittsburgh
Magee-Womens Research Institute and Foundation
204 Craft Avenue
6th Floor
Pittsburgh, PA 15213

Other Participating Researchers

Gerald Schatten, PhD - employed by University of Pittsburgh

Expected Research Outcomes and Benefits

Understanding the dynamics and molecular composition of the cell's spindle poles, the centrosomes, in normal and cancerous cells, as well as the post-translational modifications of the microtubules, affords new targets for designing chemotherapeutic strategies. This may well translate into innovative cancer treatments. This also is of keen importance for understanding the basic biology of every cell during division.

Summary of Research Completed

The Aims of this research projection have not been changed or modified during this reporting period.

Aim 1. Do cancer cells display differences in the delta-2 post-translational modification of alpha-tubulin as compared with noncancerous cells? We tested an affinity purified antibody to delta-2 (Δ-2) tubulin in non-cancerous lung fibroblast cell line (WI-38), a lung carcinoma line (NCIH292) and a breast cancer cell line (MCF7), all purchased from ATCC (Manassas, VA). WI-38 lung fibroblast were grown in Minimal Essential Media (MEM) + 10% fetal bovine serum (FBS), NCI-H292 lung carcinoma line was grown in RPMI media (inVitro, Carlsbad, CA) with 10% FBS and MCF7 breast cancer epithelial line was grown in MEM + 10% FBS with 0.01 mg/ml human insulin (Sigma, St. Louis, MO) on sterile 22mm^2 glass coverslips. After a brief rinse in warm sterile phosphate buffered saline (PBS), fixation was accomplished by plunging coverslips into cold (-20ºC) absolute methanol for 8-10 minutes followed by rehydration in PBS+ 0.5% Triton X-100 detergent (PBS-TX). After blocking for 1 hr in PBS-TX containing 10% normal goat serum, 3 mg/ml BSA, and 150 mg/ml glycine to reduce non-specific antibody

binding, fixed cell lines were incubated overnight in a cocktail of primary antibodies including Δ-2 rabbit anti-tubulin antibody (1:200), YOL134 anti-rat total tubulin antibody (1:200) and mouse 611B-1 acetylated α-tubulin (1:100) at 4ºC. Following a 30 min rinse in PBS-TX, primary antibodies were detected with a 1:100 dilution of fluorescein-conjugated goat anti-rabbit IgG, rhodamine conjugated goat anti-rat IgG and Cy5 conjugated anti-mouse IgG secondary antibodies applied for 2 hrs at 37ºC. After a penultimate rinse in PBS-TX, stained cells were mounted in an antifade (Vectashield, Vector Labs, Burlingame, CA) with DAPI for detecting DNA. All slides were examined with an A1 laser-scanning confocal microscope with a x100 Plan Fluor objective (NA=1.3) and the detection of Δ-2 tubulin, tyrosinated/detyrosinated tubulin and acetylated tubulin recorded for mitotic and interphase cells in all 3 cell lines.

Analysis of fixed and stained slides demonstrated that Δ-2 tubulin was expressed at mitotic and interphase centrioles in all cell lines tested. YOL 1/34 microtubules and the acetylated α-tubulin basically co-localized to spindle microtubules at mitosis with a more restricted staining pattern of acetylated α-tubulin at interphase. As shown in Figure 1, no distinct differences in Δ-2 tubulin or acetylated α-tubulin were observed between control (WI-38) and cancerous cell lines (NCI-H292, MCF7).

Aim 2. Using dynamic confocal imaging with a living marker for centrioles, does GFP-centrin behave aberrantly in cancer cells as compared with controls? In this reporting period, we have prepared our GFP-centrin (pEGFP-CETN2) construct generously donated by Dr. Jeffrey Salisbury (Mayo Clinic, Mn). In order to establish stably transduced GFP-centrin cells lines, we've used the ViraPower™ Lentiviral Packaging Mix (Invitrogen) to produce lentiviral particles) and are in the process of transducing control and cancer cell lines for GFP expression of centrin. We anticipate that we will have stably transduced lines within a month to begin addressing questions related to centrosome dynamics between cancerous and non-cancerous lines.

Aim 3. Do the molecules which reside at the centrosome differ between cancer cells and controls? We have explored over 13 different centrosome and centriole-specific affinity purified antibodies in WI-38, NCI H292, and MCF7 cell lines (Table 1). Both Δ-2 tubulin and 20H5 centrin antibodies localize to the centrioles in all three cell lines following fixation and processing as described in Aim 1, although the localization signal was weaker than anticipated. Nevertheless, no localization differences between noncancerous and cancerous lines was observed with the anti-centriolar antibodies, although both cancerous lines showed increases in spindle abnormalities (tripolar, tetrapolar spindles) and atypical numbers of centrioles at mitotic spindle poles compared to WI-38 cell line. We also tested various centrosome antibodies in all 3 cell lines, including three pericentrin antibodies and four different γ-tubulin antibodies. Adhering cells to coverslips were processed as described in Aim 1 except that three fixation methodologies were tested for each cell line: i. cold, absolute methanol for 8-10 mins; ii. 2% paraformaldehyde in warm PBS for 1 hr; and iii. Permeabilization in a glycerol-based extraction buffer (Buffer M) containing 8% methanol and 1% Triton X-100. The rationale for performing the Buffer M/methanol fixation protocol is to confirm and compare the patterns of centrosome/centriole markers with those observed after formaldehyde or absolute methanol fixation. Together, these provide confidence that these antibodies reliably describe a molecular characterization of the microtubule organizing centers (MTOCs) and are not fixation or labeling

artifacts. Controls for both false positive and false negative results were also performed on all cell lines. Secondary antibodies were not found to cross-react with microtubules, centrioles, chromosomes or nuclear elements, and produce very low background signals. Primary antibodies to γ-tubulin were tested at 1:300 while pericentrin antibodies were tested at 1:600. General tubulins were labeled with anti-rat YOL 1/34 and DNA detected with DAPI. Two of the four γ-tubulin antibodies (GTU 88 and T-5192) gave excellent staining in interphase and mitotic centrosomes in all 3 cell lines after formaldehyde fixation. Abnormal spindle morphologies and atypical centrosome counts (>2) at spindle poles were observed in some cancerous cell lines above that observed in control fibroblast cells (WI-38). Likewise, two of three pericentrin antibodies gave excellent centrosome detection in all 3 cell lines, with the brightest detection observed after Buffer M extraction and methanol fixation (see Fig 2). With these findings on conserved centriole and centrosome markers in control and cancerous cell lines, we are now posed to address how molecules like ninein, cenexin1, and ε-tubulin associate with the centriolar sub-distal appendages during duplication, migration, and mitotic spindle pole formation. formation.

Aim 4. Do the anticancer drugs currently used target these posttranslational modifications of alpha tubule, centrioles and/or these centrosomal molecular and can new drugs be discovered? To evaluate the effects of common chemotherapeutics on tubulin modifications and centrosome composition, we began testing well established chemotherapeutic drugs on our 3 cell lines, including cyclophosphamide (CTX), cisplatin, paclitaxel, vinblastine, and vincristine. All drugs were prepared as 10 mM stocks in DMSO and stored in frozen aliquots. Cell lines growing on coverslips were incubated in 1μM of each drug for 24 hrs prior to fixation in absolute cold methanol as described in Aim1. Control cells were incubated in DMSO solvent at an equal volume (1:10,000). Fixed cell were stained with pericentrin antibody 4448 (1:600), YOL 1/34 general anti-tubulin (1:200) and 611B-1 acetylated α-tubulin (1:100) and analyzed by confocal microscopy as described in Aim 1. For each drug treatment, we observed and recorded the mitotic index, centrosome numbers and centrosome position (split, migrated apart versus adjacent, adhering) for a minimum of 100 cells. We observed a significant increase in mitotic arrest in all cell lines after treatment with paciltaxel (taxol), vinblastine, and vincristine drugs compared to control, cisplatin and CTX (Fig. 4, top graphs). Microtubules were completely absent in all cells treated with vinblastine and vincristine (Fig. 3A-C), but significantly enhanced after paciltaxel treatment (Fig. 3D-F). Atypical centrosome counts (1, 3, 4 or more) were significantly increased after paciltaxel, vinblastine and vincristine exposure in all 3 cell lines relative to control, cisplatin and CTX treatments (Fig. 4, middle graphs). Interestingly, we also observed a large increase in paracrystalline arrays in the cytoplasm of NCI-H292 lung carcinoma cells after 1μM vincristine treatment relative to WI-38 control lung fibroblast or MCF7 breast cancer cell line exposed to 1μM vincristine (Fig. 3A-C), indicating NCI-H292 cells are more susceptible to this concentration of vincristine in vitro than for control or other cancer cells. Finally, we observed centrosome segregation to be significantly impacted after paciltaxel or vinblastine exposure in all 3 cell lines investigated (Fig. 4, bottom graphs). Curiously, vincristine did not appear to impact centrosome segregation in WI-38 cells but did show increased blocking of centrosome splitting in HCI-H292 and MCF7 cancer cells. The mechanism behind this observation is not yet known but will be investigated once we have GFP-expressing centrin lines available for live cell image analysis.

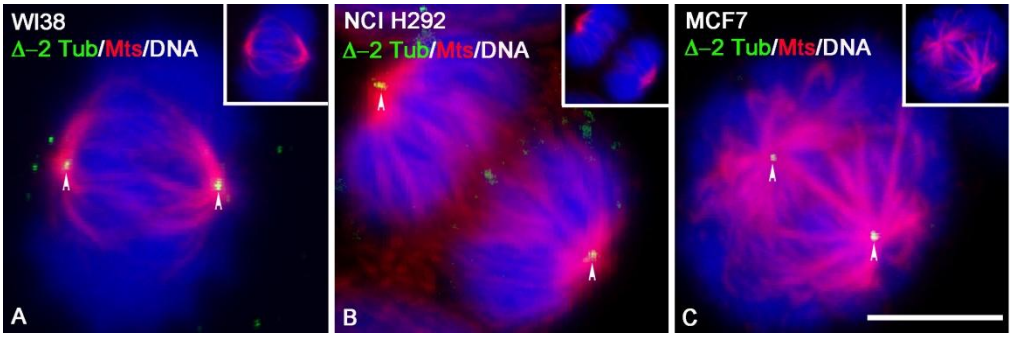

Figure 1. Delta-2 (Δ-2) Tubulin and acetylated α-tubulin detection in WI38 normal lung fibroblast, NCI H292 lung carcinoma and MCF7 breast cancer cells. Δ-2 tubulin is strongly localized to the centrioles at the spindle poles in all three lines (green, arrowheads; red, microtubules; blue, DNA). Insets: acetylated α-tubulin is largely restricted to the spindle poles (red; blue, DNA) and does not localize to the centrioles or centrosomes. All images quadruple-labeled for Δ-2 tubulin (green), general microtubules (red), DNA (blue) and acetylated α-tubulin (detected with Cy5 labeled antibody and color assigned red). Bar=10µm.

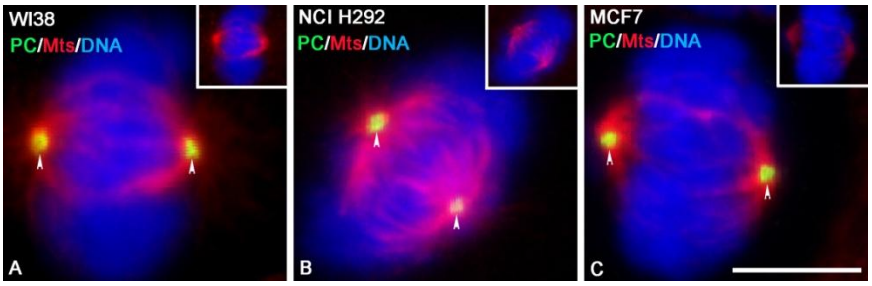

Figure 2. Pericentrin (PC) antibody 4448 and acetylated α-tubulin detection in WI38 lung fibroblast, NCI-H292 lung carcinoma, and MCF7 breast cancer cells. Pericentrin (green, arrowheads; red, microtubules; blue, DNA) is detected exclusively at the centrosome at each spindle pole in all three cell lines. Insets: acetylated α-tubulin (red) is restricted to the spindle poles (red; blue, DNA) and does not detect the centrioles. All images quadruple-labeled for pericentrin 4448 (green), general microtubules (red), DNA (blue) and acetylated α-tubulin (Cy5 antibody labeled and color assigned red). Bar=10µm.

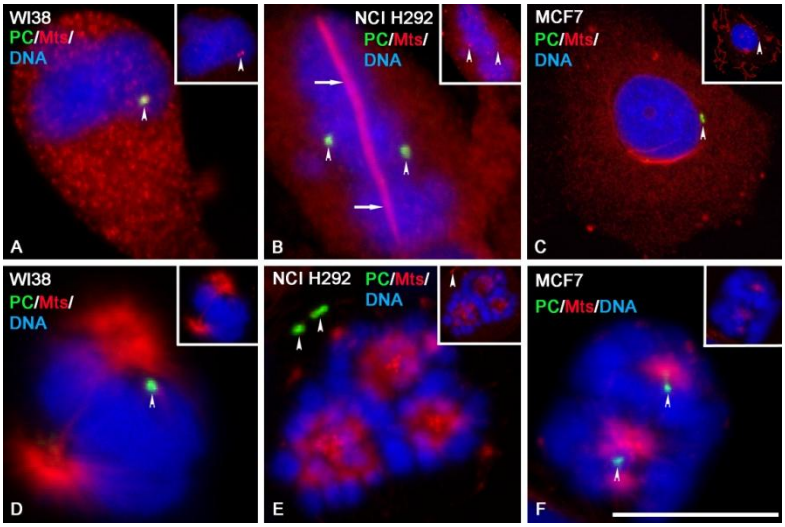

Figure 3. Pericentrin and acetylated α-tubulin in WI38, NCI-H292 and MCF7 cells after 1 µM vincristine sulfate or paciltaxel exposure for 24hrs. A-C: Cytoplasmic microtubules disassemble in the presence of vinblastine sulfate (red; blue, DNA) except for paracrystalline arrays found largely in the NCI- H292 fibroblast carcinoma cells (B: red, arrows). Pericentrin labels single (A: green, arrowhead) or duplicated centrosomes (B-C: green, arrowheads) in all 3 cell lines. Insets: acetylated α-tubulin (red, arrowheads; blue, DNA) detects centrioles in absence of assembled microtubules. D-F: Paciltaxel greatly augments spindle microtubule assembly (red; blue, DNA) while affecting centrosome numbers (A: green, arrowhead) and cytoplasmic position in most cancer cell lines (E-F: green, arrowheads). Insets: acetylated α-tubulin (red) after paciltaxel treatment detects mostly microtubules and some centrioles (E:inset, arrowhead). All images quadruple-labeled for pericentrin 4448 (green), general microtubules (red), DNA (blue) and acetylated α-tubulin (Cy5 antibody labeled and color assigned red). Bar=10µm.

Table1. Localization of Centriole and Centrosome Antibodies in Control and Cancer Cell Lines.

Antibody	Source	Type	Localization	Staining Profile in Cell Lines[1]
Delta (Δ)-2 Tubulin	Millipore, Inc	Rabbit	Centrioles	+
Centrin 20H5	Millipore, Inc	Mouse	Centrioles	+
Pericentrin1	Santa Cruz Biotechnology, Inc.	Rabbit	centrosomes	-
Pericentrin 4448	Abcam, Inc	Rabbit	Centrosomes	+++
Pericentrin 28144	Abcam, Inc	Mouse	centrosomes	++
γ-Tubulin C20	Santa Cruz Biotechnology, Inc	Goat	centrosomes	-
γ-Tubulin Tu-30	Abcam, Inc	Mouse	centrosomes	-
γ-Tubulin GTU-88	Sigma	Mouse	centrosomes	++
γ-Tubulin T-5192	Sigma	Mouse	centrosomes	++
YOL 1/34	Millipore	Rat	microtubules	+++
Acetylated 611B-1 Tubulin	Santa Cruz Biotechnology, Inc.	Mouse	Centrioles, microtubules	+++
NuMA	Compton et al	Rabbit	Spindle pole microtubules, nucleus.	+++

[1]Cell Lines tested include WI38, NCI H292, and MCF7, all from ATCC.
Key: +++: strong detection; ++: good detection; +: weak detection; -: no detection

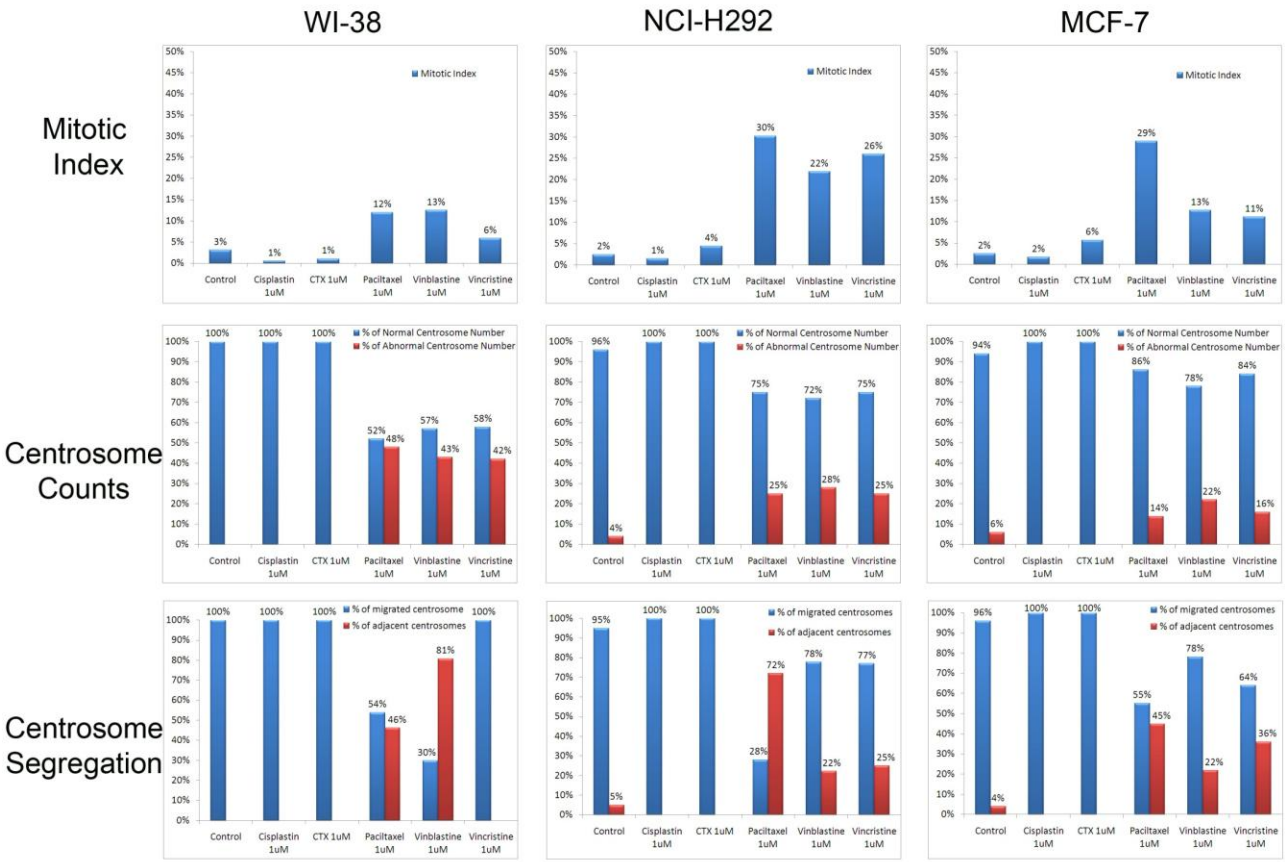

Figure 4. Graphic analysis of mitotic index, centrosome numbers and position in WI-38, NCI-H292 and MCF-7 cells after chemotherapeutic drug treatments. Top graphs: cell cycle arrest in mitosis is significantly increased in WI-38 lung fibroblast, NIC-H292 lung carcinoma, and MCF-7 breast cancer lines after treatment with 1µM paciltaxel, vinblastine sulfate or vincristine sulfate, but not cisplatin or cyclophosphamide (CTX). Middle graphs: normal detection of two centrosomes is significantly disrupted in all three cell lines after 1µM paciltaxel, vinblastine sulfate or vincristine sulfate but not cisplatin or CTX. Abnormal centrosome numbers include 1, 3, 4 or more cytoplasmic centrosomes as detected by anti-pericentrin antibody. Bottom graphs: centrosome segregation is dramatically blocked in NCI-H292 and MCF-7 cancer cell lines after 1µM paciltaxel, vinblastine sulfate or vincristine sulfate treatment but not cisplatin or CTX. Curiously, for the normal lung fibroblast line WI-38, 1µM vincristine did not show inhibition of centrosome splitting despite complete microtubule disassembly. WI-38 cells treated with 1µM paciltaxel and vinblastine sulfate did show significant effects on centrosome position within the cytoplasm.